

FIG. 1. Eastern United States, 11 October 1973, one-third nautical mile resolution.

MAJOR QUENTEN L. WILKES  
6th Weather Wing Hq.  
Andrews AFB, Maryland 20331

## Meteorology Applications of Satellite Imagery

Automated processing procedures are applied to incorporate the data into the automated cloud analysis.

*(Abstract on page 1166)*

### INTRODUCTION

THE DATA ACQUISITION and Processing Program (DAPP) of USAF (DAPP changed its name to The Defense Meteorological Satellite Program (DMSP) on 13 December 1973.) The

spectrum of applications includes meteorology, oceanography, geophysics, earth resources, and other miscellaneous interests. This presentation is confined primarily to a survey of some of the primary applications in

---

## Photo on Front Cover

*An application of AIP (Automated Imagery Processing).* Using digital change detection and other digital processing techniques, this composite image depicting both a current and a previous activity in Norfolk harbor is shown. The more recent activity is depicted by the background photograph which is reproduced digitally with 64 gray-scale shades. Previous activity is indicated by the "ghost" ships, expressed as white outlines. This image was created digitally through precise spatial and radiometric matching of the two original images, followed by application of a spatial gradient (derivative) to the previous activity image.

The creative application of the above AIP techniques and countless related others to the fields of weather, cartography, earth resources, non-destructive testing, military reconnaissance, etc., are limited only by the knowledge of how uniquely to apply AIP to the user's problem.

Original photo furnished courtesy by USAF, Rome Air Development Center; digital processing provided by Digital Image Systems Division, Control Data Corp., Minneapolis, Minn.

---

meteorology and a description of the automated processing of image data for cloud analysis at the Air Force Global Weather Central (AFGWC), Offutt AFB, Nebraska.

### APPLICATIONS IN METEOROLOGY

In meteorology the first and most extensive use of satellite imagery has been in cloud analysis. Figure 1 shows the eastern United States at a resolution of one-third nautical mile (n. mi.) on visual imagery. Across the center of the picture is a frontal cloud structure extending from Pennsylvania on the

right to Western Tennessee on the left. The amount and area of the cloud cover is easily analyzed.

In the lower part of the picture over northern Florida the character and extent of a scattered cloud area is clearly shown. On the right-hand side, over the Atlantic Ocean, the nature and extent of the cloud cover could never be constructed from surface reports alone.

Clouds not associated with classical weather systems, such as fronts and low-pressure areas, are often some of the most

---

*ABSTRACT: A survey of primary satellite imagery applications in meteorology. Applications are illustrated with examples of actual phenomena as shown by satellite imagery. Automated processing procedures are described as used at the Air Force Global Weather Central to incorporate satellite imagery data into the automated 3D-NEPH cloud analysis.*

---

interesting features and are clearly revealed by satellite imagery. An example of one such revelation is a thin line of cumulus clouds in Figure 2 which mark the edge of the subsiding and outflowing air from dissipating thunderstorms as indicated by question marks. Some meteorologists call these *crescent* cloud lines because they are usually curved. Investigations indicate their movement and location can be used to help predict where the next area of thunderstorms will break out.

Similar thin cloud lines occur from other dynamic processes. On Figure 3 these thin cloud lines spread out from Hainan Island like the bow waves of a ship. The clear area to the west of the Island is the result of subsidence (or descending air) to the lee side of the Island.

The top of Figure 4 shows a well-developed cloud system over Northern Europe. In the center are dendritic patterns of the snow-covered Alps and Pyrenees. However, in the lower part of the picture is a particularly interesting well-developed band of clouds over the middle of the Mediterranean. Again, this is an example where surface observations alone would not reveal this extensive cloud formation.

In the upper-left corner of Figure 5, along the northern coast of Spain, is a unique cloud

pattern which shows up quite brightly. This is probably a low cloud formation associated with on-shore winds. Looking down to northwest Africa one can see a band of scattered-to-broken clouds. These usually mark the presence of a local maximum of westerly winds over this area.

In the lower center of this picture is the shadow of the moon as it eclipsed the sun at the time this image was recorded. The changes in brightness of the picture near the word *Umbra* and just above it near the label 300 nm (nautical miles) are caused by a step function (Automatic Gain Control) which changes the sensor gain along the track as the satellite crosses regions of different light levels.

The location of typhoons and hurricanes from satellite imagery has become a routine procedure. Location accuracies of storms with visible eyes, such as Figure 6, have an average deviation from the official track of less than 15 n. mi. This picture of Typhoon Betty shows an irregular boundary around the eye of the storm. The next two illustrations show other characteristics of eyes of typhoons.

The picture of Typhoon Pamela (Figure 7) shows the eye covered with clouds but still identifiable. Storms like this can be located

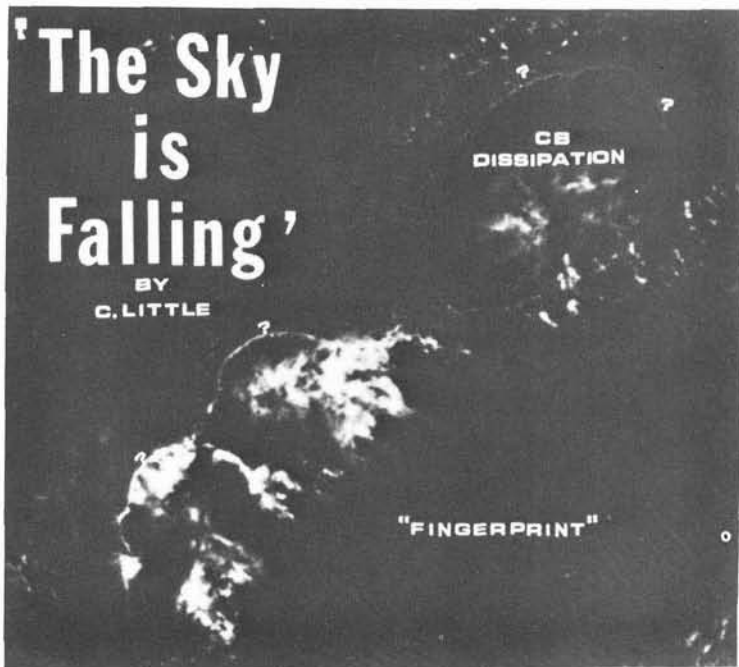


FIG. 2. Northwest of Marshall Islands, 0.4 to 1.1  $\mu\text{m}$  spectral interval, 0.3 n. mi. resolution, 5 March 1973, local noon.

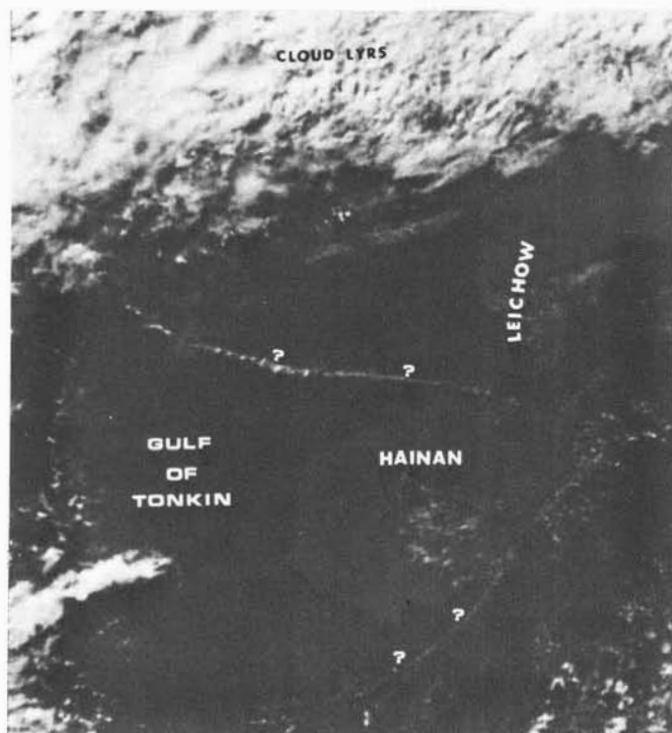


FIG. 3. Gulf of Tonkin, 0.4 to 1.1  $\mu\text{m}$  spectral interval, 0.3 n. mi. resolution.



FIG. 4. Western Mediterranean, noon (date unknown), 0.3 n. mi. resolution, 0.4 to 1.1  $\mu\text{m}$  spectral interval.

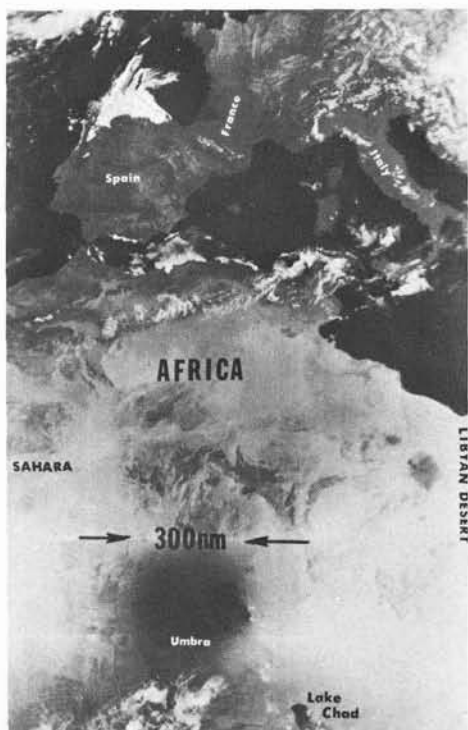


FIG. 5. North Africa, Solar Eclipse, 30 June 1973, noon, 0.3 n. mi. resolution, 0.4 to 1.1  $\mu\text{m}$  spectral interval.

with an average deviation of slightly less than 20 n. mi. Typhoon Patsy (Figure 8) shows an eye with a sloping wall.

Another application of the DMSP imagery data has been in the Space Environmental Support Section (SESS) at AFGWC (Figure 9). One of the tasks of this section is to describe the ionosphere and its changes. These are significant in radio and radar propagation which are of interest to Air Force Communications Service and Air Defense Command. These pictures of the Aurora Borealis are very useful in the ionospheric analysis. The DMSP satellite has the only sensor that has been able to produce these images in real time. This is made possible through the use of variable-gain settings in the amplification of the sensor's response. The gain is set very high when the satellite views the night side of the earth.

Figure 10 shows a large section of the Aurora Borealis with most of the city lights of northwestern Europe clearly visible. Although the best auroral images are recorded during no-moonlight nights, the high-gain setting for the visual sensor was first used to record clouds during moonlit nights.

#### AUTOMATED PROCESSING

At AFGWC, Meteorological Satellite Imagery Data are received, ingested, and applied to



FIG. 6. Typhoon Betty, 12 August 1972, morning, 0.3 n. mi. resolution, 0.4 to 1.1  $\mu\text{m}$  spectral interval.

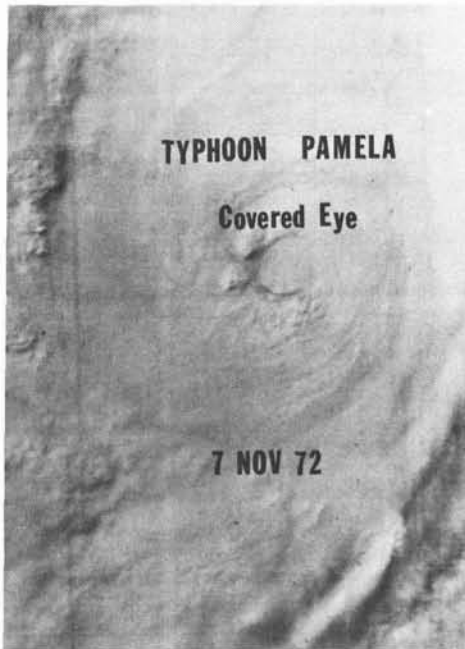


FIG. 7. Typhoon Pamela, 7 November 1972, noon, 0.3 n. mi. resolution, 0.4 to 1.1  $\mu\text{m}$  spectral interval.

cloud analysis in a fully automated mode. Data are transmitted from the satellite to ground readout stations which relay the data to AFGWC and simultaneously passes it to a data formatter and/or photo processor/display. The photo processor displays an image (cylindrical projection) on positive transparency film.

The data formatter reformats the material so that a computer can ingest it. The current data stream includes converting from analog to digital data. In the future the data stream will be in digital form. The formatter output can be recorded on magnetic tape or sent directly to a computer (UNIVAC 1110) for processing.

The output from computer processing is digital statistics and digital image data. Digital image data are passed to a display device which produces a positive transparent picture. This picture can be produced in polar stereographic or mercator projection at different scales, e.g., 1:15 million, 1:20 million, 1:30 million, and in 64 shades of gray. Digital statistics consist of an average gray shade for an area represented by a grid point and the variability of the data samples of that area.

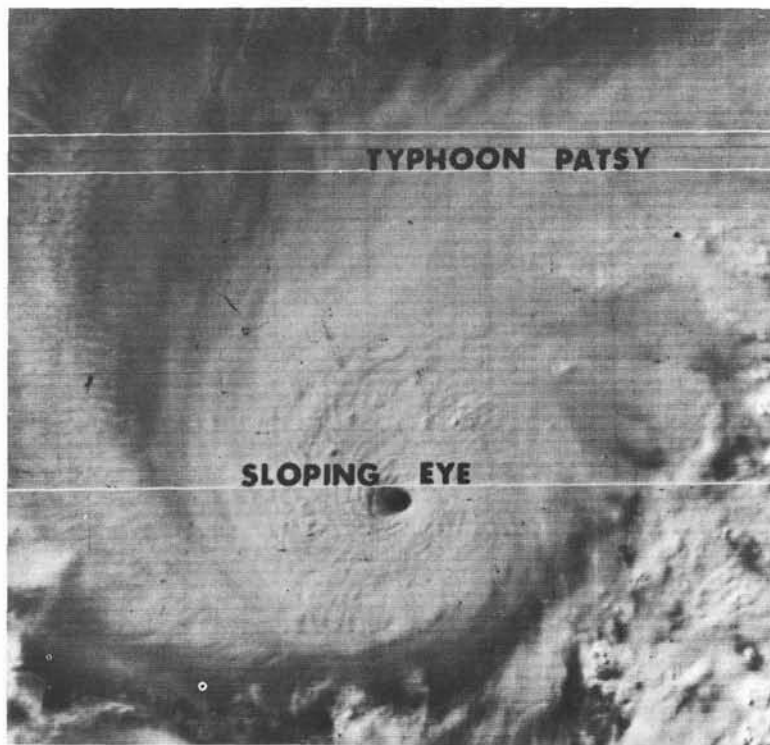


FIG. 8. Typhoon Patsy, 9 October 1973, noon, 0.3 n. mi. resolution, 0.4 to 1.1  $\mu\text{m}$  spectral interval.

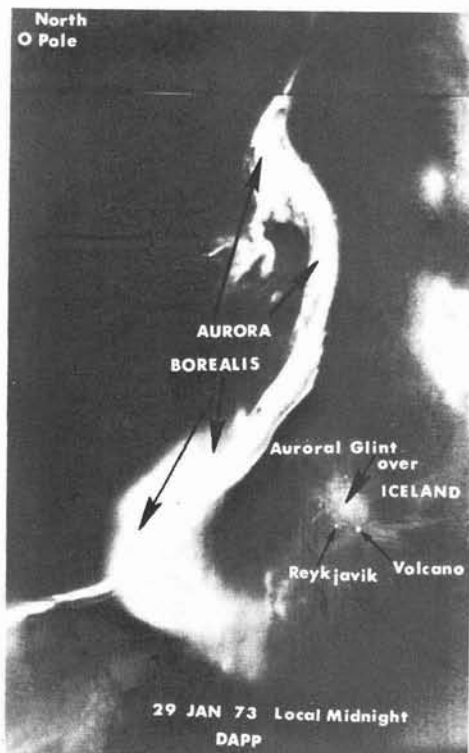


FIG. 9. Iceland Aurora, 29 January 1973, no moonlight, 2 n. mi. resolution, 0.4 to 1.1  $\mu\text{m}$  spectral interval.

These statistics are used in the three-dimensional cloud analysis 3D-NEPH program that is processed in the U-1110 computer.

The data processing function can be divided into tasks as indicated in Table 1. The satellite image is produced by a scanning radiometer. Each scan line is recorded on the spacecraft, transmitted to AFGWC, and recorded at AFGWC in sequence. Thus, processing can begin on the first scan lines received while the remaining scan lines are still being transmitted. As the data are received by the computer, they are put into a temporary mass storage file which can be accessed while it is being filled.

The extraction process consists of separating visual, infrared, and telemetry data which are multiplexed in the raw data stream (Table 2). First, data are retrieved from mass storage sequentially by scan line, identified, and the telemetry data stripped off leaving only the image data. Second, scan lines are numbered sequentially and appropriate scan lines are

TABLE 1. PRIMARY DATA PROCESSING

Extraction.
Location.
Normalization.
Application and Display.

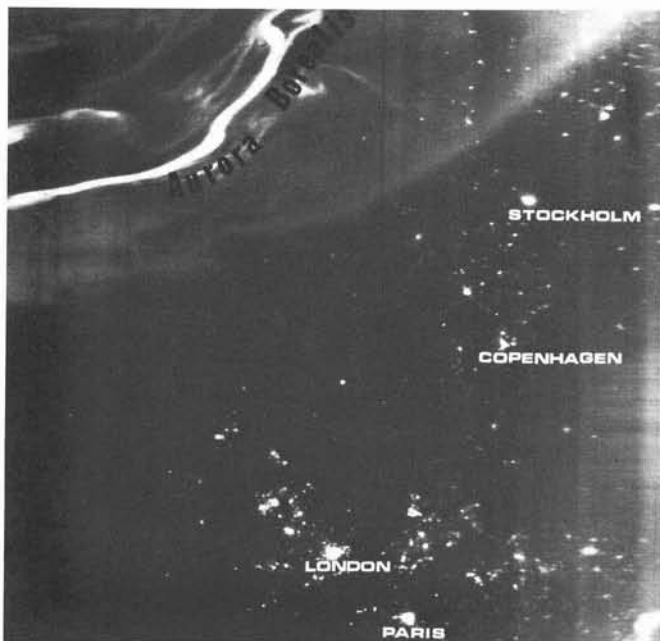


FIG. 10. Aurora, Northwest Europe, midnight, date unknown, no moonlight, 2 n. mi. resolution, 0.4 to 1.1  $\mu\text{m}$  spectral interval.

tied to time flags at two-minute intervals. Third, replacement tables, unique for each satellite/sensor, are used to fill in missing or noisy data samples within a scan line. Fourth, the video and infrared data are demultiplexed and placed in mass storage.

TABLE 2. EXTRACTION

---

Retrieve data from mass storage.  
Trim off telemetry data.  
Number scan lines sequentially.  
Fill in noisy or missing data samples.  
Demultiplex video and infrared data.  
Place in mass storage.

---

The location process consists of locating the data and transposing the information to a fixed (for any one-quarter orbit) grid (Table 3). The data are retrieved from mass storage sequentially by scan line. Location of points on a scan line is calculated from ephemeris-derived information. Scan-line locations relative to bench points on the map grid are determined. The nearest data sample is selected to provide a value for each grid point.

TABLE 3. LOCATION

---

Retrieve cleaned data from mass storage.  
Locate samples by ephemeris-derived data.  
Map data onto a fixed grid.

---

The normalization process (Table 4) consists of adjusting the grid-point sample values for the inequalities of lighting due to sun-earth-spacecraft geometric relationships. This process is performed at each grid point as soon as a data sample value has been selected.

The first step is determining sun-earth-satellite geometric and optical parameters.

TABLE 4. NORMALIZATION

---

Determine sun-vehicle earth parameters.  
Define brightness adjustments.  
Recognize sun-glint areas.  
Place data in mass storage.

---

Then brightness adjustments are defined and sun glint areas are determined. Third, the adjustment to the sample value is made. Fourth, digital statistics are calculated. Finally, the statistics and image data are put into a mass storage file.

Applications of the processed data are innumerable. Following the automated path, computed statistical data are used as the primary input to the AFGWC 3D-NEPH program, integrating surface observations, aircraft reports, radar reports, etc., to provide the best possible cloud analysis (Table 5). At AFGWC a much-used product of the processed data is the 1:15 million scale polar stereographic positive transparency or glossy print displays that are used by forecasters in a wide variety of manual applications.

TABLE 5. APPLICATION AND DISPLAY

---

$\frac{1}{8}$  GWC mesh statistics for 3D-NEPH.  
Integrated with other data.  
Best data selected—no averaging.  
Positive transparency displayed.  
Positive prints for multiple users.  
Quality control/check on processing.

---

Much of the DMSF data are unique. Thus the USAF has made arrangements with NOAA/NEWW to provide data to the scientific community. Non DoD agencies should contact Mr. David S. Johnson, Director of NESS, FOB-4, Suitland, Maryland 20233 for further information.

DoD agencies should contact Hq AWS/SY, Scott AFB, Illinois 62225; or Hq 6WW/DO, Andrews AFB, Maryland 20331.

---

## FORUM

### Cahill Papers

Dear General Jacobs:

Thanks so much for the obituary for my husband (*Photo. Engr.*, June 1974, page 742). I appreciate this so much.

I took his original mapping papers to the Smithsonian Institution at their request. They are being kept as the "Cahill Collection" under the Care of Mr. Eugene Ostaff, Curator of Photography. They will be housed in the National Museum of History & Tech-

nology. Dr. Robert M. Vogel, Curator of the Division of Mechanical and Civil Engineering, was my contact, and he is the one to whom I delivered the papers. Mr. Harry Tubis is preparing a pamphlet on my husband's work for you.

I thought that you might find all this interesting.

—Jane M. Cahill  
August 4, 1974